Supporting Information for

Stuides of Iron(III) Porphyrinates Containing Silanethiolate Ligands

Daniel J. Meininger, Jonathan D. Caranto, Hadi D. Arman, and Zachary J. Tonzetich*

Department of Chemistry, University of Texas at San Antonio, San Antonio, TX 78249

zachary.tonzetich@utsa.edu

Contents **Pages**

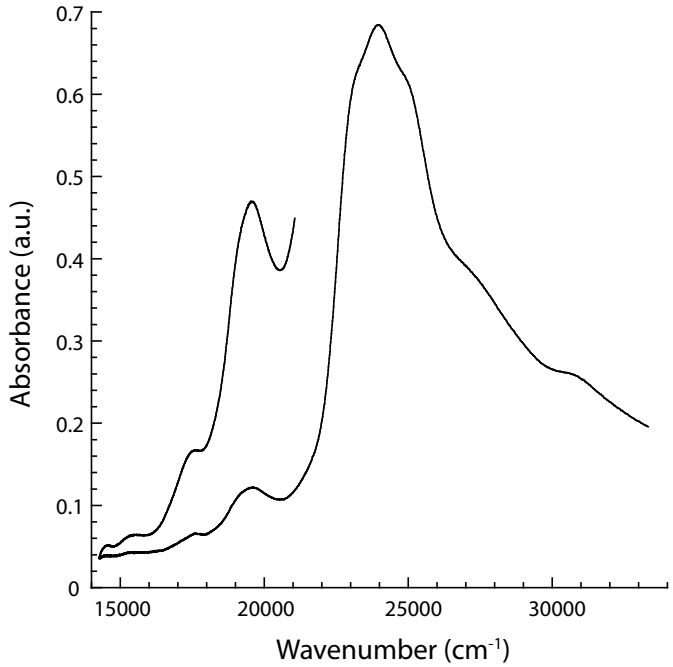

Figure S1. Electronic absorption spectrum of [Fe(STIPS)(TPP)] in dichloromethane.

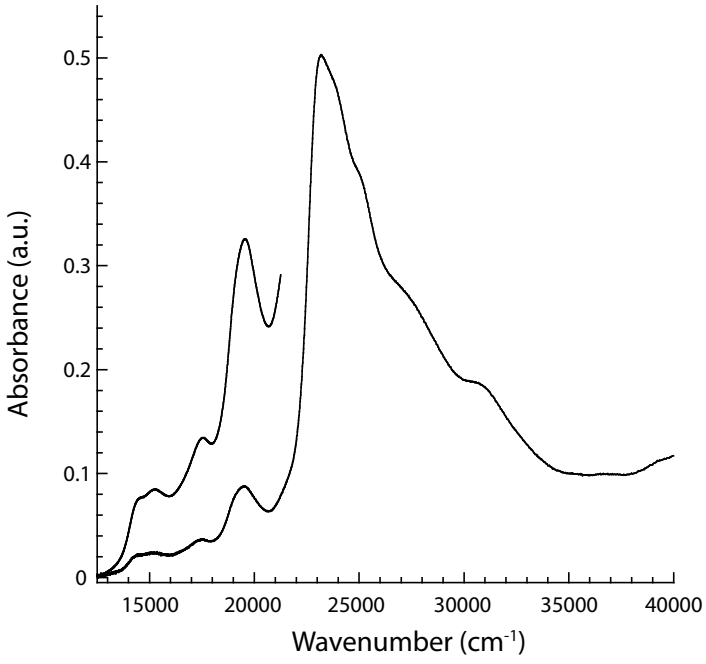

Figure S2. Electronic absorption spectrum of [Fe(STIPS)(TMP)] in dichloromethane.

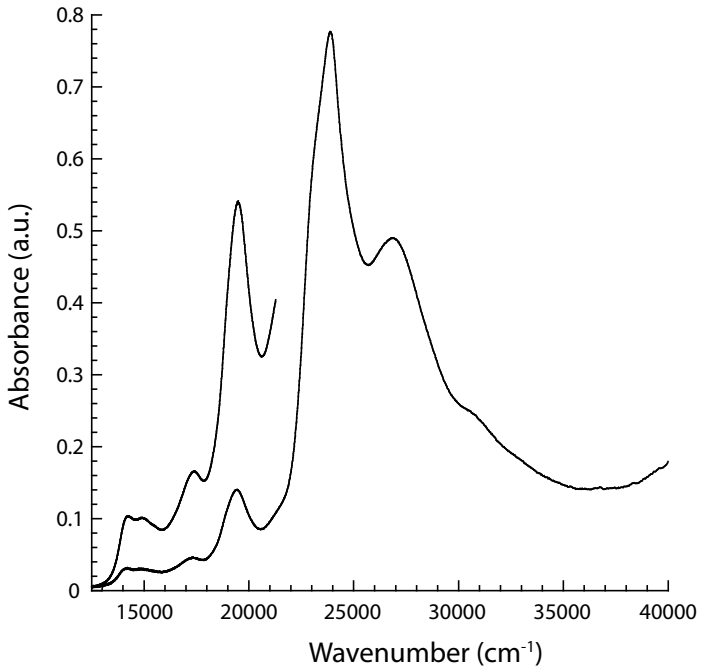

Figure S3. Electronic absorption spectrum of [Fe(SSiPh$_3$)(TMP)] in dichloromethane.

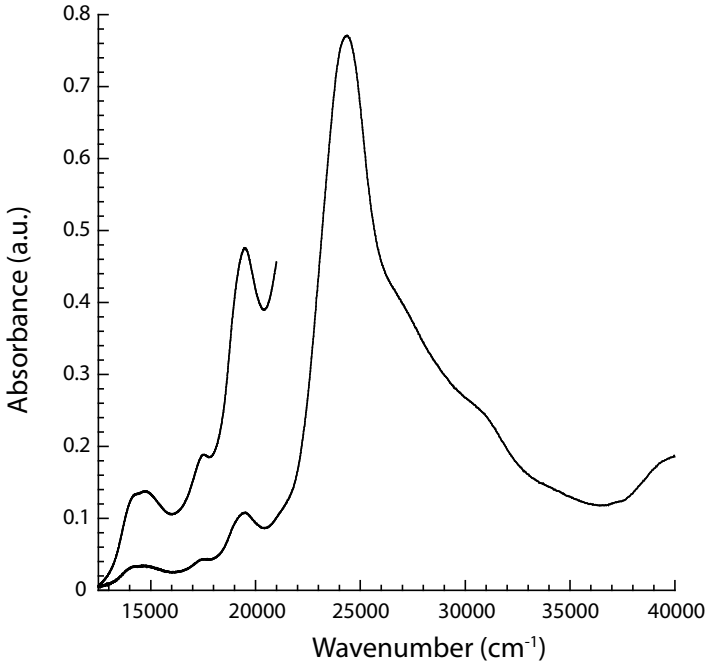

Figure S4. Electronic spectrum of [Fe(SPh)(TMP)] in dichloromethane.

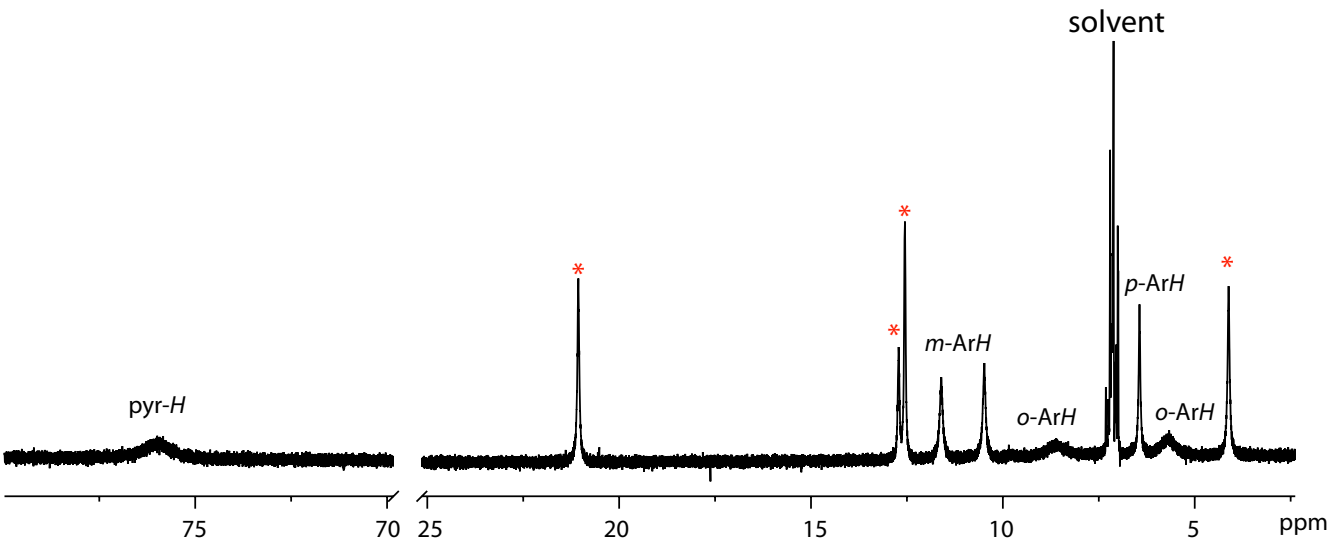

Figure S5. 500 MHz ^{1}H NMR spectrum of the reaction of [Fe(OMe)(TPP)] and ^{t}BuSH in benzene-d_6. Red asterisks denote peaks due to [Fe^{II}(TPP)].

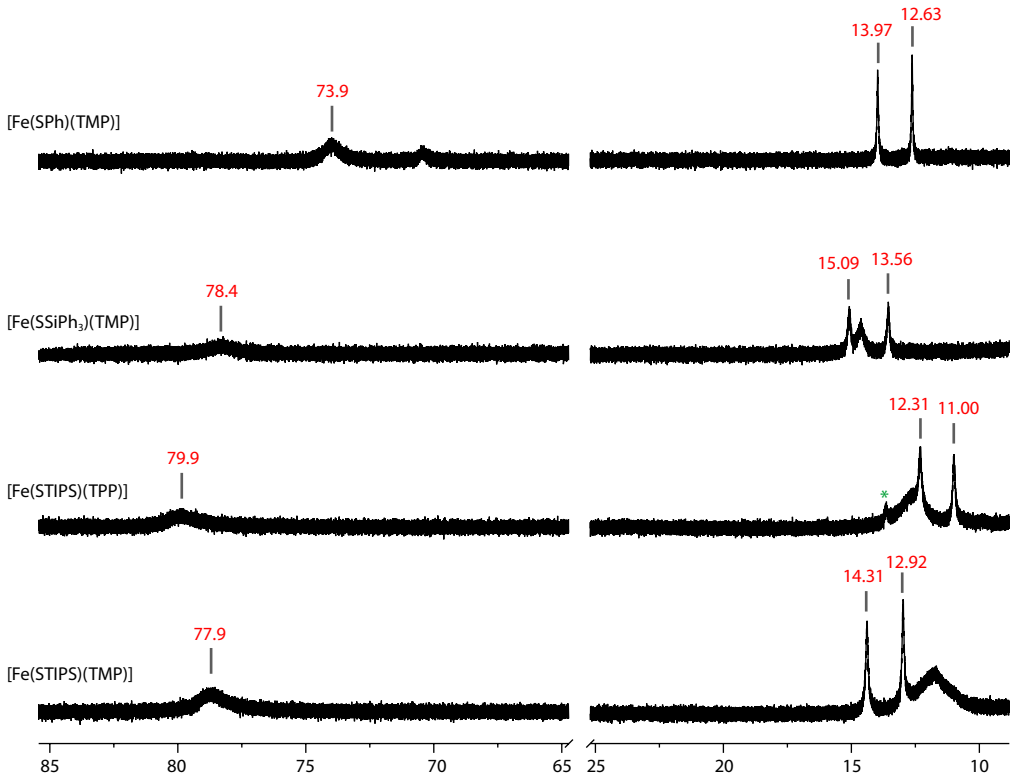

Figure S6. Pyrrolic and *m*-Ar region of the 500 MHz ^{1}H NMR spectra (benzene-d_6) for several iron(III) porphyrinates containing sulfur ligands. The green asterisk in the spectrum of [Fe(STIPS)(TPP)] corresponds to a minor impurity, most likely [Fe^{II}(TPP)].

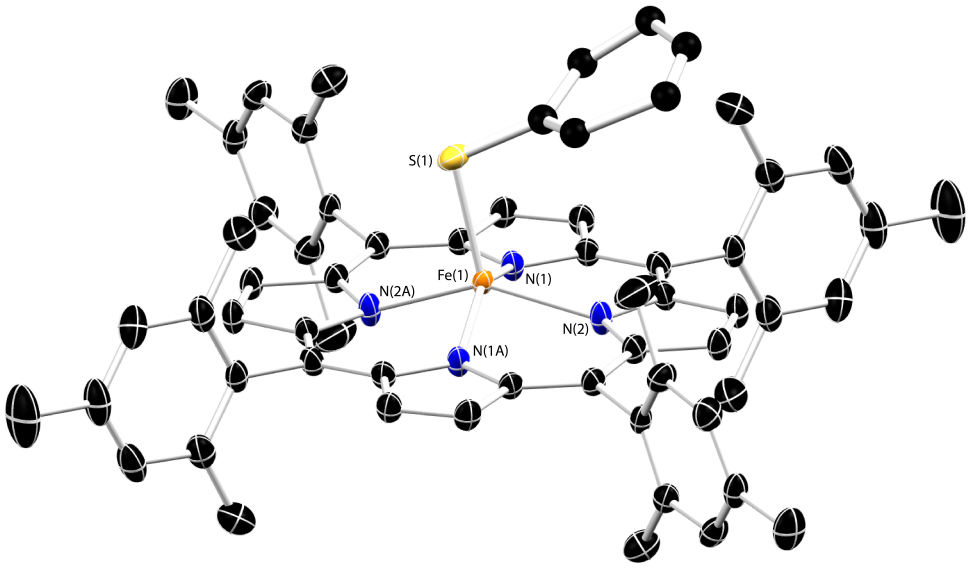

Figure S7. Depiction of the solid-state structure of [Fe(SPh)(TMP)] showing the geometry and connectivity of the atoms.

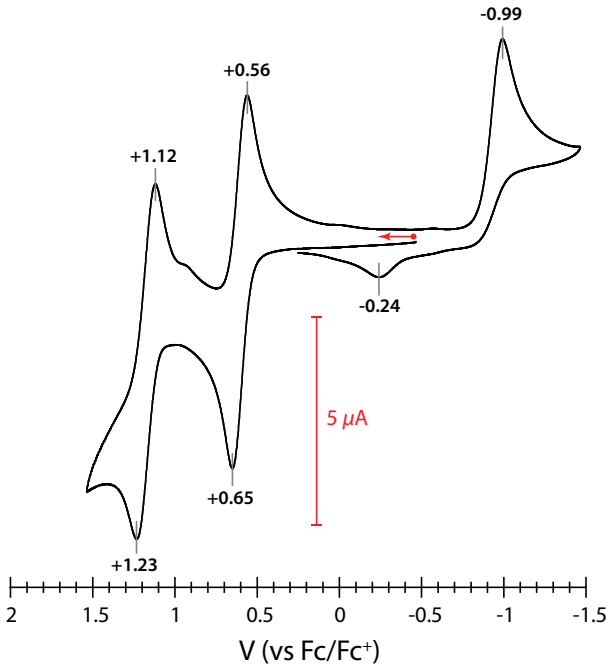

Figure S8. Cyclic voltammogram of [FeCl(TMP)] at a Pt disk electrode in CH_2Cl_2 displaying two reversible oxidation events centered at +1.18 V and +0.61 V, and an irreversible reduction event at −0.99 V. The small event at −0.24 V observed in the return wave is likely due to oxidation of a species formed by chloride dissociation from $[FeCl(TMP)]^-$. Scan rate is 50 mV/s and the supporting electrolyte is 0.1 M Bu_4NPF_6.

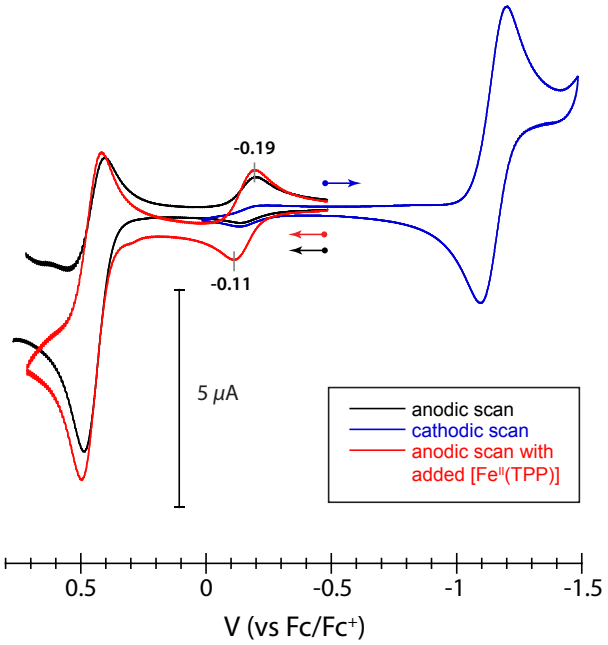

Figure S9. Cyclic voltammogram of [Fe(STIPS)(TPP)] at a Pt disk electrode in CH_2Cl_2. Depicted are the anodic and cathodic scans comprising Figure 4 of the text and the effect of added [Fe^{II}(TPP)]. Scan rate is 50 mV/s and the supporting electrolyte is 0.1 M Bu_4NPF_6.

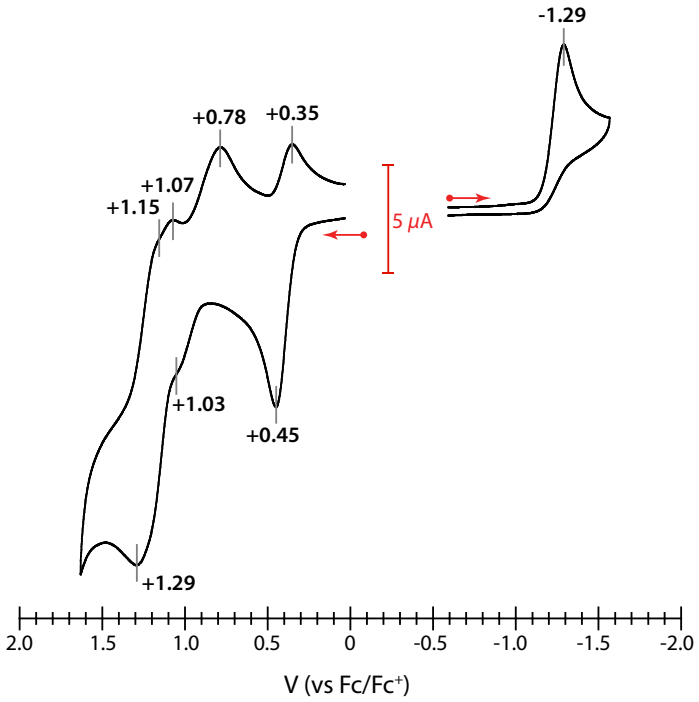

Figure S10. Cyclic voltammogram of [Fe(STIPS)(TMP)] at a Pt disk electrode in CH_2Cl_2. Scan rate is 50 mV/s and the supporting electrolyte is 0.1 M Bu_4NPF_6.

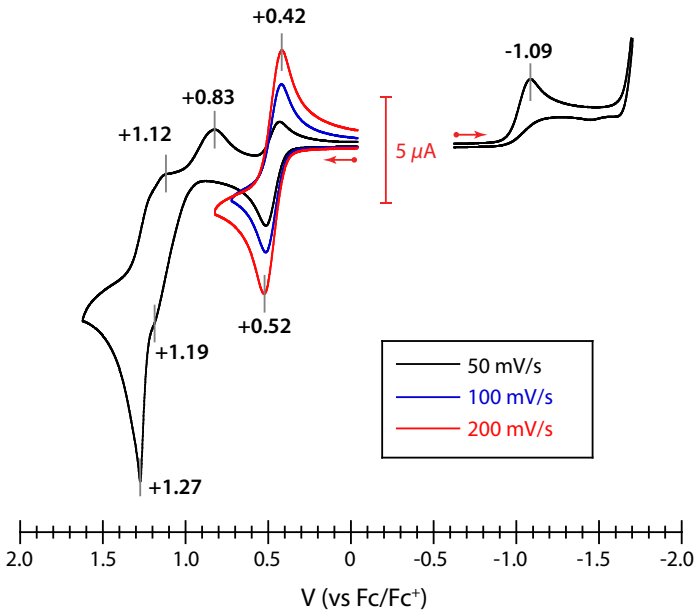

Figure S11. Cyclic voltammogram of [Fe(SSiPh$_3$)(TMP)] at a Pt disk electrode in CH_2Cl_2. Scan rate is 50 mV/s and the supporting electrolyte is 0.1 M Bu_4NPF_6.

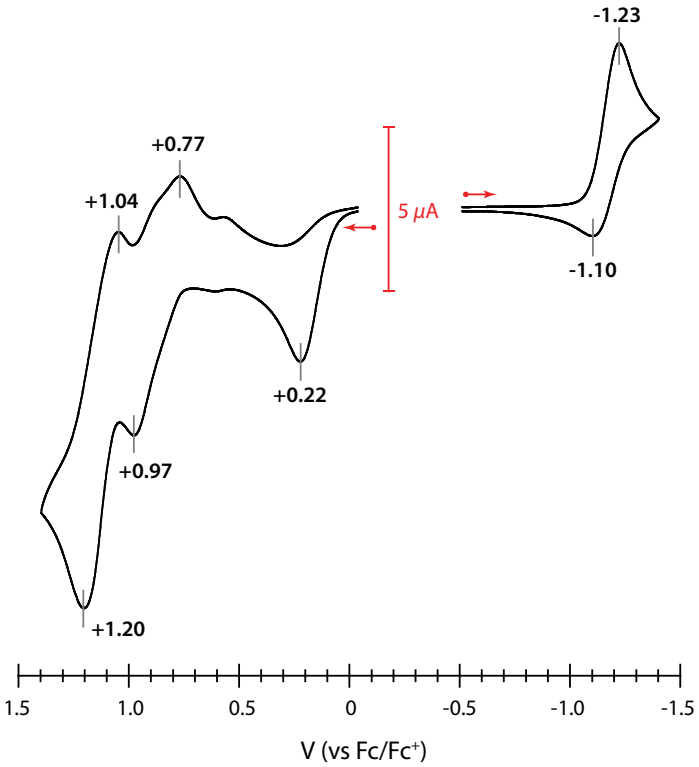

Figure S12. Cyclic voltammogram of [Fe(SPh)(TMP)] at a Pt disk electrode in CH_2Cl_2. Scan rate is 50 mV/s and the supporting electrolyte is 0.1 M Bu_4NPF_6.

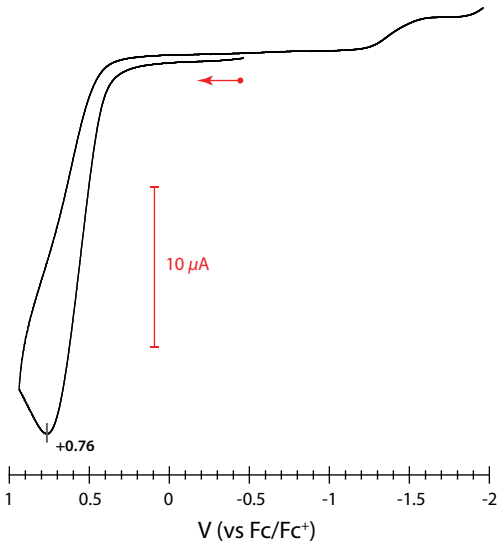

Figure S13. Cyclic voltammogram of $HSSi^{i}Pr_3$ at a Pt disk electrode in CH_2Cl_2 in the presence of excess Et_3N displaying the oxidation of free $^{-}SSi^{i}Pr_3$. Scan rate is 50 mV/s and the supporting electrolyte is 0.1 M Bu_4NPF_6. The potentials are referenced to an external ferrocene/ferrocenium couple.

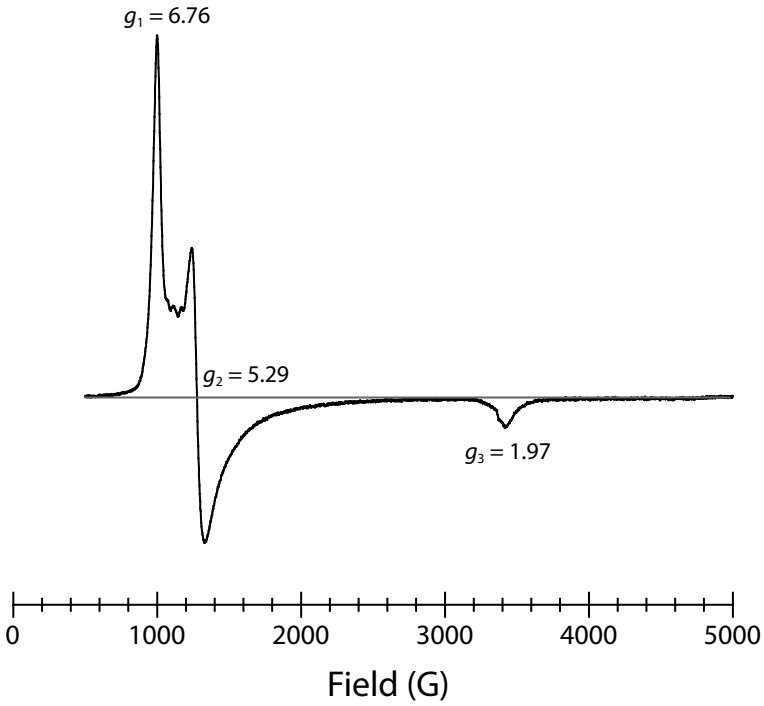

Figure S14. EPR spectrum of [Fe(STIPS)(TMP)] in a 2-MeTHF glass at 77 K; $E/D = 0.0323$.

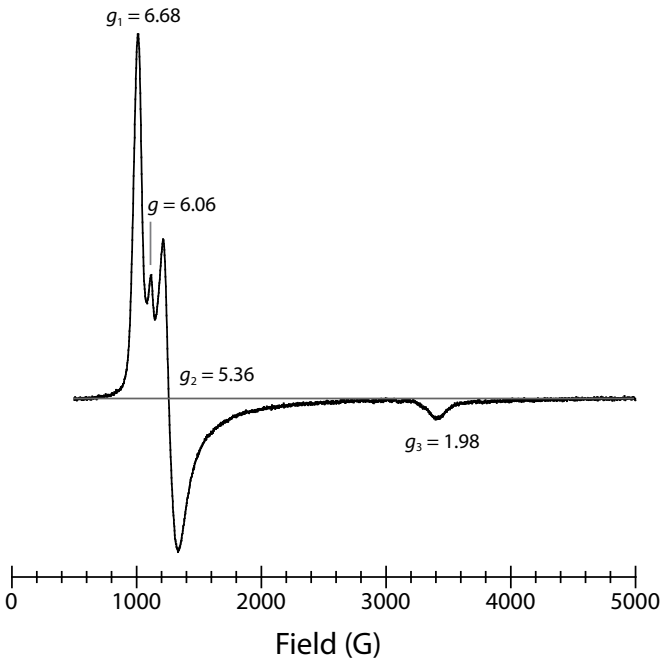

Figure S15. EPR spectrum of [Fe(SSiPh$_3$)(TMP)] in a 2-MeTHF glass at 77 K; $E/D = 0.0297$.

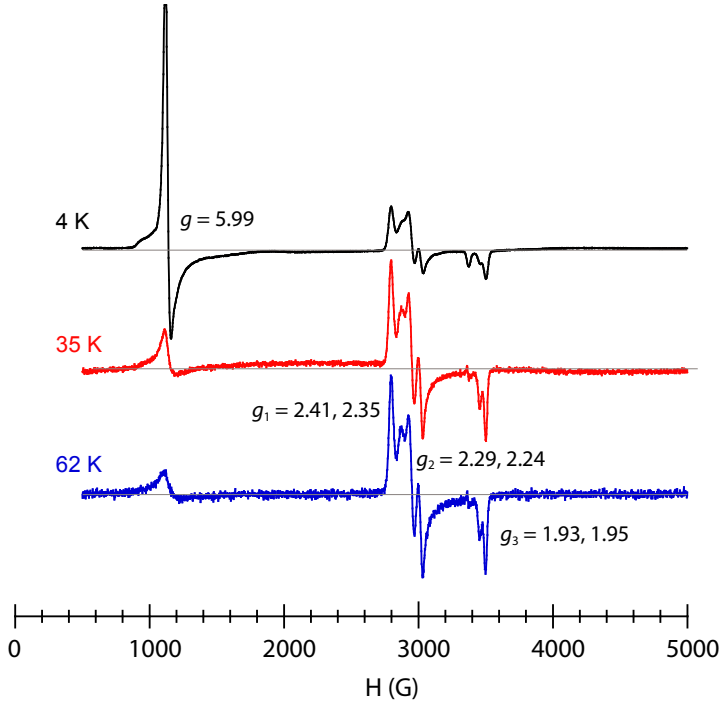

Figure S16. EPR spectra of [Fe(SPh)(TMP)] in a 2-MeTHF glass at several temperatures between 4 and 62 K showing a decrease in the low field $S = {}^5/_2$ signal ($E/D = 0.0026$) and growth of the high field signals ($S = {}^1/_2$) as the temperature increases.

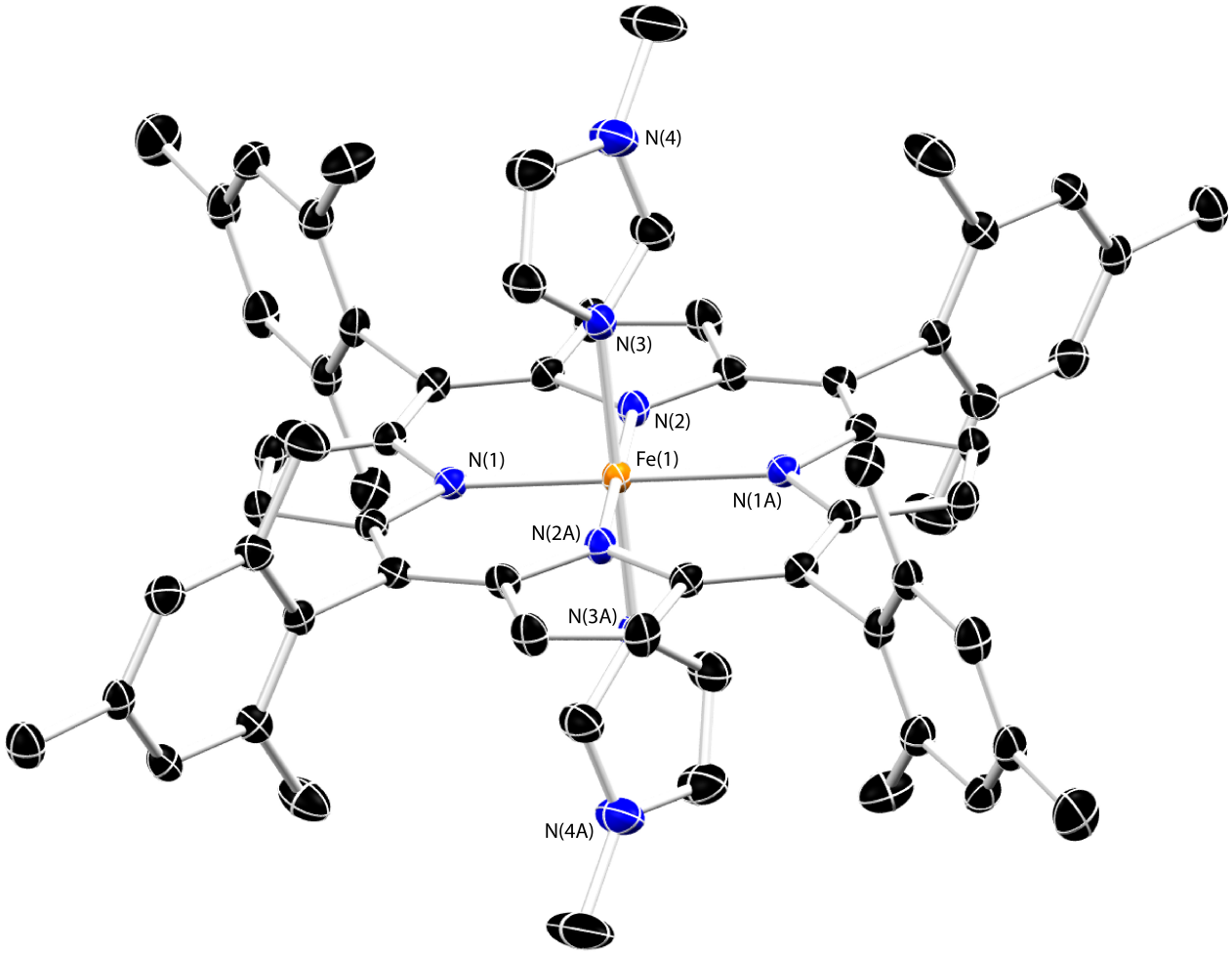

Figure S17. Thermal ellipsoid (50%) drawing of the structure of [Fe(1-MeIm)$_2$(TMP)]. Hydrogen atoms and cocrystallized benzene molecules omitted for clarity. Selected bond lengths (Å) and angles (deg): Fe(1)-N(1) = 1.990(2); Fe(1)-N(2) = 1.991(2); Fe(1)-N(3) = 1.992(2); N(3)-Fe(1)-N(3A) = 180.0(2).

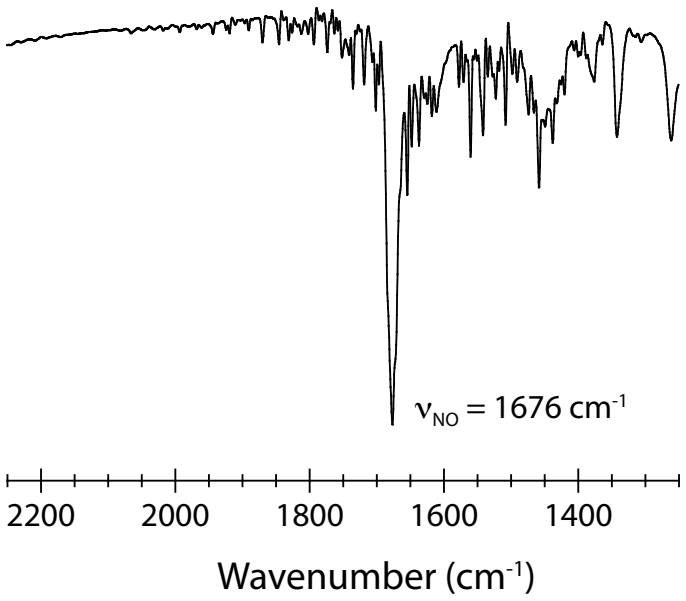

Figure S18. IR (KBr) spectrum of the product obtained from the reaction of [Fe(STIPS)(TMP)] and NO (*g*).

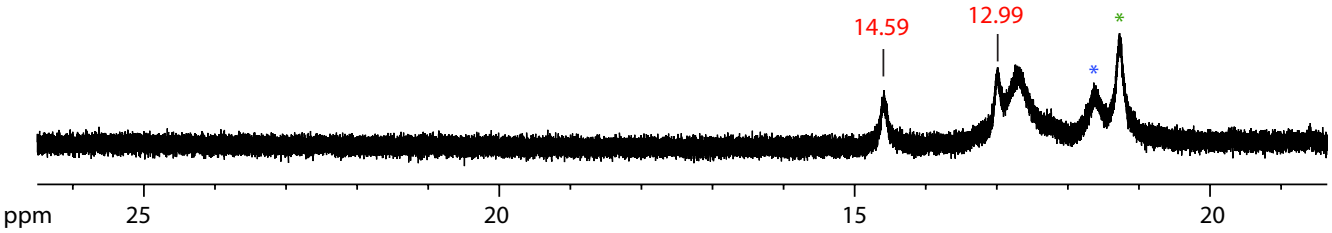

Figure S19. *m*-Ar region of the 500 MHz ^{1}H NMR spectrum of the reaction of [FeF(TMP)] with $Me_3SSiSMe_3$ in benzene-d_6. Note the resemblance of the peaks indicated in red with those in Figure S6. Asterisks denote resonances due to the starting material (blue) and [Fe^{II}(TMP)] (green).

Table S1. Crystallographic data and refinement parameters for iron porphyrinates.[‡]

Compound	**[Fe(STIPS)(TPP)]**	**[Fe(STIPS)(TMP)]**	**[Fe(SSiPh$_3$)(TMP)]**	**[Fe(1-MeIm)$_2$(TMP)]**
Empirical formula	$C_{53}H_{49}FeN_4SSi\cdot\frac{1}{2}C_6H_6$	$C_{65}H_{73}FeN_4SSi\cdot C_5H_{12}$	$C_{74}H_{67}FeN_4SSi\cdot CH_2Cl_2$	$C_{64}H_{64}FeN_8\cdot 2(C_6H_6)$
Formula weight (g/mol)	897.02	1098.42	1196.26	1229.36
Temperature (K)	98(2)	98(2)	98(2)	98(2)
Crystal system, space group	Triclinic, $P\bar{1}$	Triclinic, $P\bar{1}$	Monoclinic, $P2_1/n$	Orthorhombic, $Pcca$
Unit cell dimensions (Å, deg)	a = 11.113(3) b = 12.600(3) c = 16.927(4) α = 80.693(11) β = 85.049(12) γ = 77.332(11)	a = 13.4086(5) b = 14.4072(7) c = 17.3566(12) α = 110.724(8) β = 102.571(7) γ = 95.034(7)	a = 16.4254(13) b = 18.9508(14) c = 22.8901(19) β = 108.668(8)	a = 23.0929(16) b = 14.8314(10) c = 19.2077(11)
Volume (Å^3)	2278.9(10)	3010.6(3)	6750.2(9)	6578.6(7)
Z	2	2	4	4
Calculated density (g/cm^3)	1.307	1.155	1.177	1.241
Absorption coefficient (mm^{-1})	0.446	0.347	0.379	0.282
F(000)	944	1117	2514	2600
Crystal size (mm)	0.14 × 0.12 × 0.10	0.36 × 0.35 × 0.06	0.20 × 0.07 × 0.05	0.19 × 0.09 × 0.07
Θ range	2.2 to 26.0º	3.1 to 25.1º	3.0 to 23.1º	3.1 to 25.1º
Limiting indices	$-13 \le h \le 13$, $-14 \le k \le 15$, $-20 \le l \le 20$	$-15 \le h \le 15$, $-17 \le k \le 16$, $-18 \le l \le 20$	$-18 \le h \le 17$, $0 \le k \le 20$, $0 \le l \le 25$,	$-27 \le h \le 26$, $-13 \le k \le 17$, $-22 \le l \le 22$
Reflections collected / unique	13515 / 8871 [R_{int} = 0.0435]	17753 / 10578 [R_{int} = 0.0263]	9440 / 9440	33972 / 5821 [R_{int} = 0.0556]
Completeness to Θ	99.1%	99.3%	99.3%	99.8%
Absorption correction	multi-scan ABSCOR	multi-scan ABSCOR	multi-scan ABSCOR	multi-scan ABSCOR
Min. and max transmission	0.777 and 1.000	0.467 and 1.000	0.362 and 1.000	0.751 and 1.000
Data / restraints / parameters	8871 / 2 / 568	10578 / 0 / 676	9440 / 0 / 757	5821 / 0 / 412
Goodness-of-fit on F^2	1.008	1.018	1.034	1.029
Final R indices [I > 2σ(I)]	R_1 = 0.0587, wR_2 = 0.1288	R_1 = 0.0561, wR_2 = 0.1447	R_1 = 0.0900, wR_2 = 0.1813	R_1 = 0.0517, wR_2 = 0.1251
R indices (all data)	R_1 = 0.0687, wR_2 = 0.1358	R_1 = 0.0603, wR_2 = 0.1471	R_1 = 0.1424, wR_2 = 0.1982	R_1 = 0.0697, wR_2 = 0.1349
Largest diff. peak and hole (e·Å^{-3})	0.604 and −0.627	0.998 and −0.464	1.167 and −0.818	0.534 and −0.422

[‡]Refinement method was full-matrix least-squares on F^2; wavelength = 0.71073 Å. $R_1 = \sum||F_o|-|F_c||/\sum|F_o|$; $wR_2 = \{\sum[w(F_o^2-F_c^2)^2]/\sum[w(F_o^2)^2]\}^{1/2}$.